solvent, and the type of complex is now available from this combination of X-ray, NMR, and calculational data. These data can serve as a basis for understanding the chiral recognition observed when the alkaloids are used as resolving agents, help to elucidate details of asymmetric synthesis, and make predictions subject to experimental verification.

Experimental Section

Energy calculations and total energy minimizations were performed with the CHEMX[18] and MODEL molecular modeling programs on VAX 11/750 and 11/785 computers. MODEL is a modified and updated version of C. Still's program, written by K. Steliou, University of Montreal (1988). To obtain the energetically preferable conformations we used Allinger's MM2P[19] and MMX[20] minimization algorithms until the root-mean-square of the gradient of the energy was less than 0.01 kcal/Å. All calculations were performed by using a dielectric constant of 1.5. The NMR experiments were performed on Varian VXR-300, XL-300, and Gemini-300 spectrometers. The NMR spectra were obtained at ambient temperatures and the alkaloid concentrations were 0.02 M. All the alkaloid derivatives were prepared by literature procedures. Because of the low equilibrium constant between free and osmium-bound alkaloid, it had to be ensured that complete complexation had taken place before analyzing the NMR spectra of the osmium–alkaloid complexes. For that purpose, small amounts of osmium tetraoxide were gradually added to the alkaloid and the $\Delta\delta$ values were plotted against the total osmium tetroxide concentration. An asymptotic curve was obtained, which leveled off when maximum complexation had been reached. The NMR experiments were then performed at this point. A similar approach was applied in the study of protonation on the quinuclidine nitrogen. X-ray structure determination of (*p*-chlorobenzoyl)dihydroquinidine (**1**): Suitable crystals for X-ray structure determination were obtained from solution of **1** in a minimum amount of acetonitrile. Data were collected on a Enraf-Nonius CAD 4 defractometer. The structure was solved and refined by standard procedures. Crystallographic data are summarized in Table II.

Acknowledgment. J.S.S. and K.B.S., respectively, thank the Royal Norwegian Council for Scientific and Industrial Research, and the John Simon Guggenheim Memorial Foundation for fellowships. G.D.H.D. expresses thanks for the use of the services of the Dutch CAOS-CAMM center under Grant SON-11-20-700 and STW-NCH-440703. Modeling and computer facilities were provided by Royal Dutch Shell.

Supplementary Material Available: Tables of crystallographic data (for **1**), ^{1}H NMR data (for **1** and **5**), energy calculations for the substituted quinine and quinidine compounds, and an ORTEP drawing and tables of bond distances and bond angles (for **1**) (36 pages). Ordering information is given on any current masthead page.

An ENDOR Study of the Tyrosyl Free Radical in Ribonucleotide Reductase from *Escherichia coli*

Christopher J. Bender,[†,‡] Margareta Sahlin,[§] Gerald T. Babcock,[*,†] Bridgette A. Barry,[†,∥] T. K. Chandrashekar,[†,⊥] Scott P. Salowe,[#] JoAnne Stubbe,[#,∞] Björn Lindström,[⊖] Leif Petersson,[⊛] Anders Ehrenberg,[⊛] and Britt-Marie Sjöberg[§]

Contribution from the Department of Chemistry, Michigan State University, East Lansing, Michigan 48824, Department of Molecular Biology, University of Stockholm, Stockholm S-10691, Sweden, Department of Biochemistry, University of Wisconsin—Madison, Madison, Wisconsin 53706, National Board of Health and Welfare, Department of Drugs, Uppsala S-75125, Sweden, and Department of Biophysics, University of Stockholm, Stockholm S-10691, Sweden. *Received February 22, 1989*

Abstract: Tyrosyl radicals have been identified as components of several proteins whose function is redox chemistry. Ribonucleotide reductase is representative of this class of enzymes as its B2 subunit contains a tyrosine residue that is necessarily a radical for activity. The EPR spectrum of the immobilized enzyme is broadened, however, and only limited information can be extracted from an analysis of its line shape. In this situation, ENDOR spectroscopy is a higher resolution technique, and we used it to characterize the enzyme-bound radical in detail. ENDOR enhancement in ribonucleotide reductase is observed only at temperatures below 110 K due to a temperature-dependent relaxation enhancement of the radical by a μ-oxo-bridged pair of high-spin ferric ions. Below this temperature, excellent spectra are obtained and specific deuteration of the tyrosine residues in the protein was used to assign measured hyperfine tensors to the various protons in the radical. An analysis of the principal tensor components of the ortho protons ($A_x = -26.9$ MHz, $A_y = -7.8$ MHz, $A_z = -19.7$ MHz) and the strongly coupled β-methylene proton establishes that the radical has characteristics of a seven-member odd-alternate species with a spin density distribution of 0.16 (phenol oxygen), 0.26 (ortho), −0.07 (meta), −0.03 (ring carbon carrying phenol oxygen), and 0.49 (para). These calculations also provide a determination of the McConnell Q value for ring protons in this class of radical. The β protons are situated with dihedral angles of 30° and 90° with respect to the p_z orbital on carbon-1 of the aromatic ring. The results indicate that the tyrosyl radical of ribonucleotide reductase is uncharged and not hydrogen bonded to donors in its environment within the protein.

Ribonucleotide reductase is an essential enzyme that catalyzes the direct reduction of ribonucleotides to their corresponding deoxyribonucleotides. In a strictly regulated reaction all four ribonucleotides compete for the same enzyme active site, and accordingly the protein provides a balanced supply of precursors for DNA synthesis in living cells.[1] One fascinating feature of several ribonucleotide reductases is the presence of a stable tyrosyl free radical.[2] This type of enzyme is found in some bacteria, eukaryotic cells, and it is also coded for by certain bacteriophages and eukaryotic viruses.[3]

[†] Michigan State University.
[‡] Present address: Department of Molecular Pharmacology, Albert Einstein College of Medicine, 1300 Morris Park Avenue, Bronx, NY 10461.
[§] Department of Molecular Biology, University of Stockholm.
[∥] Present address: Department of Biochemistry, University of Minnesota, St. Paul, MN 55108.
[⊥] Present address: Department of Chemistry, Indian Institute of Technology, Kampur, India.
[#] University of Wisconsin—Madison.
[∞] Present address: Department of Chemistry, Massachusetts Institute of Technology, Cambridge, MA 02139.
[⊖] National Board of Health and Welfare.
[⊛] Department of Biophysics, University of Stockholm.

(1) Lammers, M.; Follman, H. *Struct. Bonding (Berlin)* **1983**, *54*, 29. Reichard, P. *Annu. Rev. Biochem.* **1988**, *57*, 349.
(2) Gräslund, A.; Sahlin, M.; Sjöberg, B.-M. *Environ. Health Persp.* **1985**, *64*, 139. Stubbe, J. *Biochemistry* **1988**, *27*, 3893.

0002-7863/89/1511-8076$01.50/0

The prototype for this enzyme, which has been characterized in great detail, is present in the bacterium *Escherichia coli*. It is a complex of two nonidentical subunits, denoted as proteins B1 and B2. The active site of the enzyme contains redox-active dithiols localized in protein B1 and the tyrosyl radical of protein B2. The tyrosyl radical is stabilized by an adjacent binuclear iron site. The active form of protein B2 is a homodimer of molecular weight 87 kDa (375 amino acid residues per polypeptide chain[4]), which carries one tyrosyl radical and the antiferromagnetically coupled high-spin ferric iron pair bridged by an exogenous μ-oxo ligand[5] and, presumably, also by one or two protein-derived μ-carboxylate(s).[6]

The tyrosyl radical is spontaneously generated upon air oxidation of the ferrous form of B2, a process which also generates the ferric iron center.[7] The radical has been identified as an oxidized form of tyrosine residue 122 in one of the two otherwise identical polypeptide chains of protein B2.[8] EPR and paramagnetic susceptibility data indicate that each B2 molecule, which is a peptide homodimer, contains only one tyrosyl radical.[5a,c] From experiments with B2 heterodimers in which one of the polypeptide chains carries a Tyr 122 to Phe mutation, it has been concluded that for forming an active enzyme it is sufficient that one Tyr 122 in the dimeric B2 is available for oxidation.[9] The tyrosyl radical can be reduced by the radical scavenger hydroxyurea[10] or by the addition of 1 equiv of dithionite in the presence of a suitable mediator.[7] These reactions leave the ferric iron center intact. ApoB2, which lacks both the iron center and the tyrosyl radical, can be reconstituted by addition of ferrous iron in the presence of air,[5a,10] yielding both the ferric iron center and the tyrosyl radical of active B2.

The importance of tyrosyl radicals in biological systems has become evident in the last few years. Since the discovery of this unique feature in ribonucleotide reductase,[11] tyrosyl radicals have also been found in the photosynthetic water splitting system[12] and in prostaglandin synthase.[13] In photosystem II the kinetically competent Y_Z radical, which participates in the electron transfer from the site of water oxidation to the reaction center, is the radical form of tyrosine 161 in the D1 polypeptide.[12] In prostaglandin H synthase the radical has been proposed to abstract a hydrogen from C-13 of arachidonate, yielding a C-13 localized radical which can then undergo the cyclooxygenase reaction.[13]

EPR provides a useful means by which to characterize these naturally occurring radical species, and the tyrosyl radical in protein B2 from *E. coli*, as well as that from bacteriophage T4, has been studied in some detail by this technique.[8a,14] The two major hyperfine couplings that occur in the ribonucleotide reductase radical and the protons responsible for these couplings have been identified in these studies. Less strongly coupled protons, however, cannot be resolved owing to the spectral broadening that occurs in these powder spectra. ENDOR provides a means by which to extract additional information from these powder EPR spectra as the spectral complexity in ENDOR increases additively with hyperfine interaction, not multiplicatively, as with EPR. Moreover, the ENDOR spectrum provides a direct measure of the principal components of each hyperfine tensor. In the work reported here, we used this technique to characterize the tyrosyl radical of ribonucleotide reductase in more detail. Hyperfine tensors of the ring protons have been determined and these assignments have been confirmed by using enzyme samples that contain specifically deuterated tyrosines or have been reconstituted in deuterium buffer. Analysis provides information on unpaired electron spin densities, radical geometry, and the occurrence of hydrogen-bonded protons. In a second paper,[12e] the results of an ENDOR study of the stable tyrosine radical that occurs in photosynthetic systems will be reported. The results obtained help to rationalize the striking differences in EPR line shape that is observed for these two naturally occurring radicals.[8,12,14]

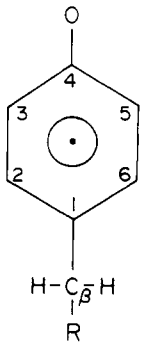

Figure 1. Numerical assignments of carbons on the tyrosyl aromatic residue.

Experimental Section

Materials. L-[3,5-^{2}H]tyrosine and D,L-[β,β-^{2}H]tyrosine were prepared as described elsewhere.[15] D_2O, 99.97% pure, was obtained from Studsvik Energiteknik AB, Sweden. Tris buffer in D_2O was prepared by freeze-drying a stock solution of 1 M Tris·HCl, pH 7.6, and dissolving it in D_2O. The freeze-drying procedure was repeated three times.

Protein Preparations. Active protein B2[16] was prepared from the overproducing strain *E. coli* C600/pBS1 as described earlier.[17] Specifically deuterated protein B2 was prepared from cells grown in Davis minimal medium[18] containing L-[3,5-^{2}H]tyrosine or DL-[β,β-^{2}H]tyrosine, as described earlier for the overproducing strain KK546.[19] To obtain optimal growth conditions a balanced supply of nondeuterated amino acids was added to the medium (0.025–0.2 g·L^{-1} medium). Removal of the iron by chelation and reconstitution of the B2 sample in D_2O was performed as described by Atkin et al.,[10] except that stock solutions of lithium 8-hydroxyquinoline-5-sulfonate and imidazole were freeze-dried and then dissolved in D_2O. The freeze-drying procedure was repeated twice. Hydroxylamine was dissolved directly in the deuterated chelation mixture. The D_2O reconstituted sample was prepared as follows: 200 μL of protein B2 (2.5 mM, in 50 mM Tris·HCl buffer in D_2O, pH 7.6) was dialyzed against a deuterated chelation solution of 10 mL containing 50 mM lithium 8-hydroxyquinoline-5-sulfonate and 1 M imidazole, pH 7.0, and 30 mM hydroxylamine hydrochloride. Desalting and concentration after the chelation procedure were performed with a Centricon

(3) Slabaugh, M.; Roseman, N.; Davis, R.; Mathews, C. *J. Virol.* **1988**, *62*, 519.
(4) Carlson, J.; Fuchs, J. A.; Messing, J. *Proc. Natl. Acad. Sci. U.S.A.* **1984**, *81*, 4294.
(5) (a) Petersson, L.; Gräslund, A.; Ehrenberg, A.; Sjöberg, B.-M.; Reichard, P. *J. Biol. Chem.* **1980**, *255*, 5706. (b) Sjöberg, B.-M.; Loehr, T. M.; Sanders-Loehr, J. *Biochemistry* **1982**, *21*, 96. (c) Sahlin, M.; Petersson, L. Gräslund, A.; Ehrenberg, A.; Sjöberg, B.-M.; Thelander, L. *Biochemistry* **1987**, *26*, 5541.
(6) Backes, G.; Sahlin, M.; Sjöberg, B.-M.; Loehr, T. M.; Sanders-Loehr, J. *Biochemistry* **1989**, *28*, 1923.
(7) Sahlin, M.; Gräslund, A.; Petersson, L.; Ehrenberg, A.; Sjöberg, B.-M. *Biochemistry* **1989**, *28*, 2618.
(8) (a) Sjöberg, B.-M.; Reichard, P.; Gräslund, A.; Ehrenberg, A. *J. Biol. Chem.* **1978**, *253*, 6863. (b) Larsson, A.; Sjöberg, B.-M. *EMBO J.* **1986**, *5*, 2037.
(9) Larrson, A.; Karlsson, M.; Sahlin, M.; Sjöberg, B.-M. *J. Biol. Chem.* **1988**, *263*, 17780.
(10) Atkin, C. L.; Thelander, L.; Reichard, P.; Lang, G. *J. Biol. Chem.* **1973**, *248*, 7464.
(11) Ehrenberg, A.; Reichard, P. *J. Biol. Chem.* **1972**, *247*, 3485.
(12) (a) Barry, B. A.; Babcock, G. T. *Proc. Natl. Acad. Sci. U.S.A.* **1987**, *84*, 7099. (b) Debus, R. J.; Barry, B. A.; Babcock, G. T.; McIntosh, L. *Proc. Natl. Acad. Sci. U.S.A.* **1988**, *85*, 427. (c) Debus, R. J.; Barry, B. A.; Sithole, I., Babcock, G. T.; McIntosh, L. *Biochemistry* **1988**, *27*, 9071. (d) Vermaas, W. F. J.; Rutherford, A. W.; Hansson, O. *Proc. Natl. Acad. Sci. U.S.A.* **1988**, *85*, 8477. (e) Bender, C. J.; Rodriguez, I. D.; Chandrashekar, T. K.; El-Deeb, M.; O'Malley, P. J.; Barry, B. A.; Babcock, G. T., *in preparation*.
(13) Karthein, R.; Dietz, R.; Nastainczyk, W.; Ruf, H. H. *Eur. J. Biochem.* **1988**, *171*, 313. Kulmacz, R. J.; Tsai, A.-L.; Palmer, G. *J. Biol. Chem.* **1987**, *262*, 10524. Dietz, R.; Nastainczyk, W.; Ruf, H. H. *Eur. J. Biochem.* **1988**, *171*, 321. Prince, R. C. *Trends Biochem. Sci.* **1988**, *13*, 286.
(14) Sahlin, M.; Gräslund, A.; Ehrenberg, A.; Sjöberg, B.-M. *J. Biol. Chem.* **1982**, *257*, 366.
(15) Lindström, B.; Sjöqvist, B.; Anggard, E. J. *Labelled Compd.* **1974**, *10*, 187. Achenbach, H.; König, F. *Chem. Ber.* **1972**, *105*, 784.
(16) For nomenclature, see: Sahlin et al., ref 7.
(17) Salowe, S. P.; Stubbe, J. *J. Bacteriol.* **1986**, *165*, 363. Sjöberg, B.-M.; Hahne, S.; Karlsson, M.; Jörnvall, H.; Göransson, M.; Uhlin, B. E. *J. Biol. Chem.* **1986**, *261*, 5658.
(18) Davis, B. D.; Mingoli, E. S. *J. Bacteriol.* **1950**, *60*, 17.
(19) Sjöberg, B.-M.; Reichard, P.; Gräslund, A.; Ehrenberg, A. *J. Biol. Chem.* **1977**, *252*, 536.

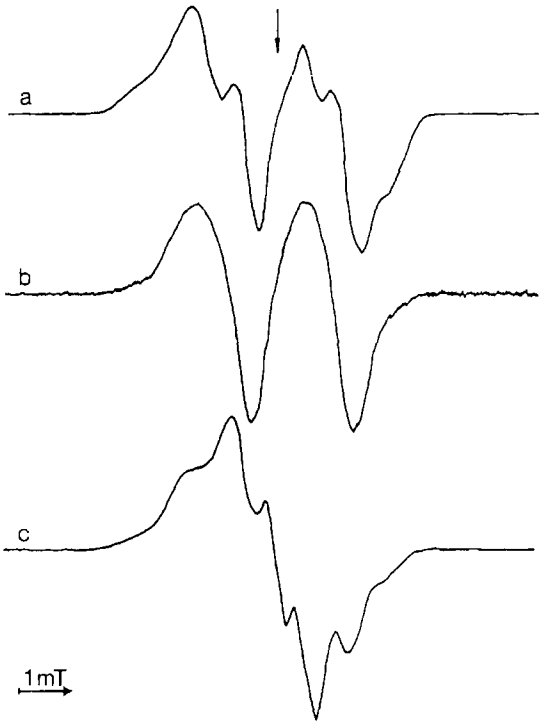

Figure 2. EPR spectra of tyrosyl free radical in ribonucleotide reductase from *E. coli* at 10 K under nonsaturating conditions: (a) cells grown in normal medium, (b) cells grown in a medium containing [3,5-^{2}H]tyrosine, and (c) cells grown in medium containing [β,β-^{2}H]tyrosine. The arrow indicates $g = 2.0047$. All spectra were recorded with a 100-kHz modulation, 0.14-mT width, and a microwave power of 0.2 μW.

30 filter device (Amicon).[20] To regenerate the iron-radical center, freshly prepared $Fe(NH_4)_2SO_4 \cdot 6H_2O$ in deaerated D_2O was added to apoB2. The amount of added ferrous iron corresponded to 2.4 times the protein concentration. This yielded a concentration of 1.1 mM protein B2 and 1.0 mM tyrosyl radical, as judged from the light absorption spectrum.

EPR Measurements. EPR first-derivative spectra were recorded at X-band on a Bruker ESP300 equipped with an ST-8701 multipurpose cavity. A temperature of 10 K was achieved with an Oxford Instruments helium flow cryostat (ESR900).

ENDOR Measurements. ENDOR spectra were recorded at X-band by using a Bruker ER200D series spectrometer equipped with an ER250 ENDOR/triple accessory and ER250ENB cavity. The spectrometer is controlled by a Nicolet 1180 data system. Radiofrequency power is supplied to a helical ENDOR coil from an ENI 3100L amplifier driven at frequencies generated by a Wavetek (3000-446) synthesizer.

The ENDOR coil that was used consists of 18 turns of silver wire and is a modified version of a previously published design.[21] Our unit differs from this published design in that much of the brass in the fittings used to make electrical contact was cut away to reduce stray capacitance. Coil and cavity are fitted to an Oxford Instruments continuous flow cryostat (ESR900) and, thus configured, the cavity has an estimated Q of approximately 800. The impedance of the radio-frequency circuit is 50 Ω and was matched when necessary with impedance transformers that were built in our laboratory following a design by Ruthroff.[22] The g value and free proton resonant frequency were determined from direct measurement of magnetic field strength and microwave frequency. For these measurements a Bruker ER035M NMR gaussmeter and a Hewlett-Packard 5245 counter/5255 3-12 GHz converter were used.

Results

Changes in the EPR spectrum of ribonucleotide reductase have been observed previously when the tyrosyl radical was generated in cells that had been grown in a medium that contained specifically deuterated tyrosine.[8a] The present samples reproduce the EPR properties of those reported earlier, which were constrained to an identification of the major couplings from the [3,5] protons and the C-β protons (see Figure 1 for the ring numbering system used here). Typical EPR spectra are shown in Figure 2.

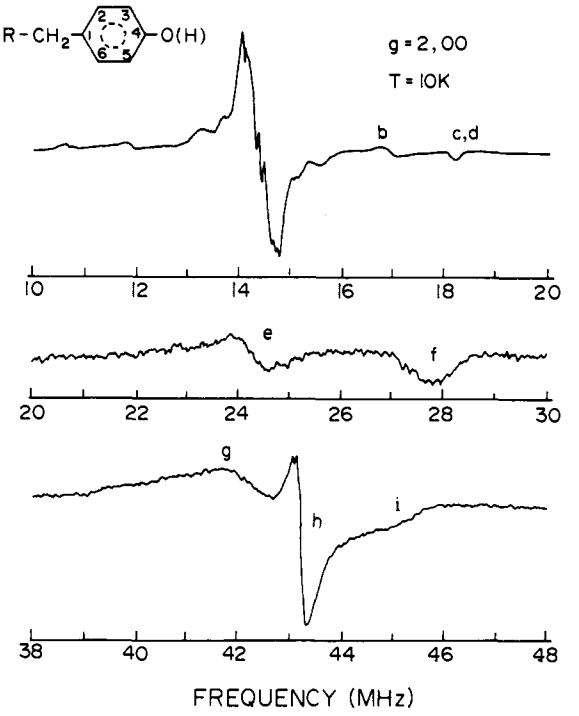

Figure 3. Proton ENDOR spectrum of ribonucleotide reductase. Letters associated with transitions correspond to those listed in Table I. Spectrometer conditions: microwave power, 3 mW; radiofrequency power, 70 W; FM amplitude, 30 kHz (10–20-MHz range), 75 kHz (>20 MHz). $\nu_p = 14.36$ MHz.

Observation of the ENDOR effect is contingent upon the relaxation properties of the radical. Experiments with ribonucleotide reductase are complicated by the interaction between the tyrosyl radical and the antiferromagnetically coupled iron center that is composed of a μ-oxo-bridged pair of high-spin ferric ions.[5] The magnetic interaction between the radical and the nearby iron pair enhances the spin–lattice relaxation rate and increases the EPR line width of the organic free radical. This interaction compelled us to perform the ENDOR experiments at low temperature despite the fact that EPR spectra can be obtained even at room temperature. Below 30 K, $(T_1T_2)^{-1}$ of the tyrosyl radical in the enzyme isolated from bacteria and the free tyrosyl radical become equivalent. Above 30 K μ_{eff} of the binuclear iron center rapidly increases, and dipolar interaction occurs between the radical and the iron center to produce enhanced relaxation of the former.[5c] We found that the optimal temperature for ENDOR was 10 K, and that the upper limit for observing any ENDOR effect at all was 110 K.

The proton ENDOR spectrum of the native enzyme, Figure 3, is interpreted from the corresponding ENDOR spectra of the enzyme isolated from cells grown on specifically deuterated tyrosine. In Figures 4 and 5, the effects of tyrosine deuteration at the [3,5] ring and β-methylene proton positions, respectively, upon the ENDOR spectrum are illustrated. From these spectra it is apparent that the transitions observed in the frequency range 20–30 MHz arise from the [3,5] protons, and the feature centered at 43 MHz corresponds to the β-methylene protons. The ENDOR transitions are labeled alphabetically in Figure 3, and Table I lists the transition frequency of each feature indicated in the spectrum.

In the earlier EPR work on specifically deuterated tyrosine, an isotropic coupling of 7.5 G (21 MHz) for the [3,5] protons was deduced.[14] The ENDOR couplings we observe for this set of protons are in the same range and correspond to the principal hyperfine tensor components of their interaction with the unpaired electron spin. The observation of these turning points is a unique advantage of using ENDOR and allows us to deduce both the isotropic and anisotropic components of the [3,5] ring proton

(20) Sjöberg, B.-M.; Sanders-Loehr, J.; Loehr, T. M. *Biochemistry* **1987**, *26*, 4242.
(21) Hurst, G.; Kraft, K.; Schultz, R.; Kreilick, R. *J. Magn. Reson.* **1982**, *49*, 159.
(22) Ruthroff, C. L. *Proc. IRE* **1959** (August), 1337.

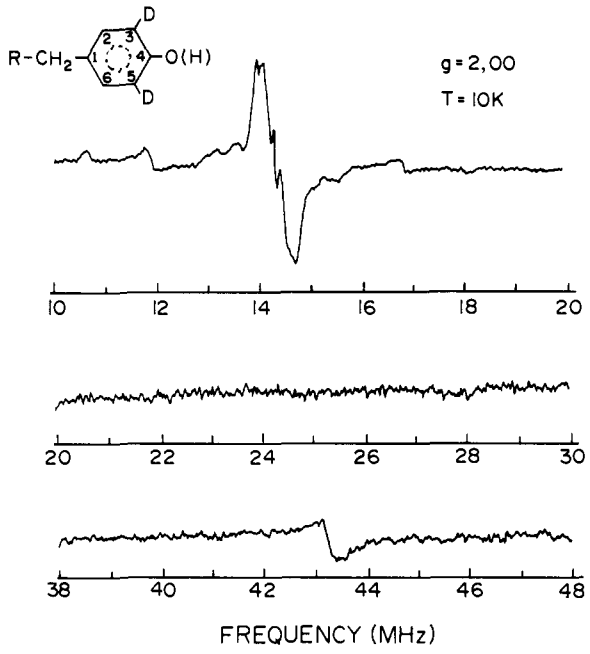

Figure 4. Proton ENDOR spectrum of ribonucleotide reductase into which has been incorporated [3,5-^{2}H]tyrosine. Assignment to the [3,5] protons of the transitions in the 20–30-MHz region is based on these data (spectrometer conditions as in Figure 3).

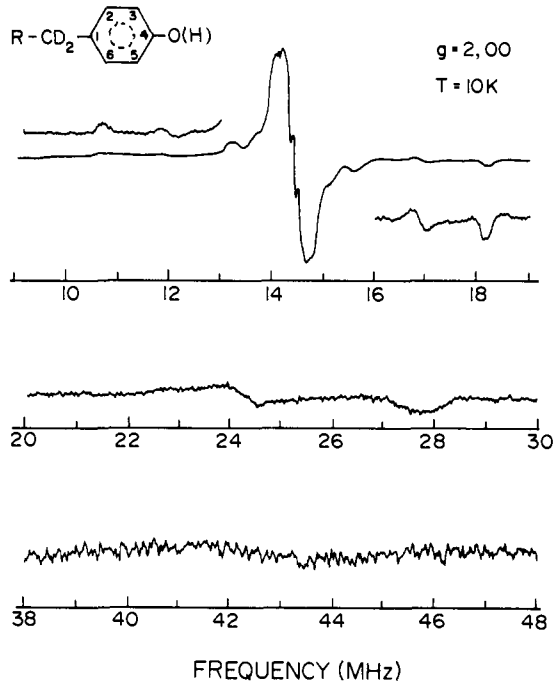

Figure 5. Proton ENDOR spectrum of ribonucleotide reductase containing tyrosine deuterated at the β-methylene position, on which is based the assignment of the high-frequency transitions (spectrometer conditions as in Figure 3).

tensor. For this class of protons (i.e., an α-proton), one often obtains a rhombic principal hyperfine tensor component pattern of $^1/_2A_{iso}$, A_{iso}, $^3/_2A_{iso}$.[22,23] These three values correspond to the A_y, A_z, and A_x hyperfine tensor components, respectively, in an axis system in which the y axis is along the C–H bond and the z axis is parallel to the axis of the p_z orbital, i.e., perpendicular to the plane of the ring. In our spectra we assign the transitions at 24.3 and 27.8 MHz to A_z and A_x of the [3,5] protons, respectively. These transitions correspond to hyperfine couplings

(23) McConnell, H. M.; Heller, C.; Cole, T.; Fessenden, R. W. *J. Am. Chem. Soc.* **1960**, *82*, 766.

Table I. ENDOR Transitions and Their Assigned Couplings

transition	ν, MHz	proton	tensor component	coupling constant, MHz
a_1	15.4[a]	β-methylene	A_z	−1.9
a_2	15.9[a]	β-methylene	A_x	−2.3
a_3	16.9[a]	β-methylene	A_y	+4.2
b	16.8	[2,6] proton	A_1	+4.8
c	18.2	[2,6] proton	A_2	+7.6
d	18.3	[3,5] proton	A_y	−7.8
e	24.3	[3,5] proton	A_z	−19.7
f	27.8	[3,5] proton	A_x	−26.9
g	41.8	β-methylene	A_y	+54.8
h	43.2	β-methylene	A_z	+57.8
i	44.8	β-methylene	A_x	+60.8
j	42.2[b]	β-methylene	$A_\parallel$	+54.8
k	44.5[b]	β-methylene	$A_\perp$	+59.4

[a] Determined from Figure 9. [b] Determined from Figure 7, axial line. [c] $A/2 = \nu_p \pm \nu$. [d] $\nu = A/2 \pm \nu_p$.

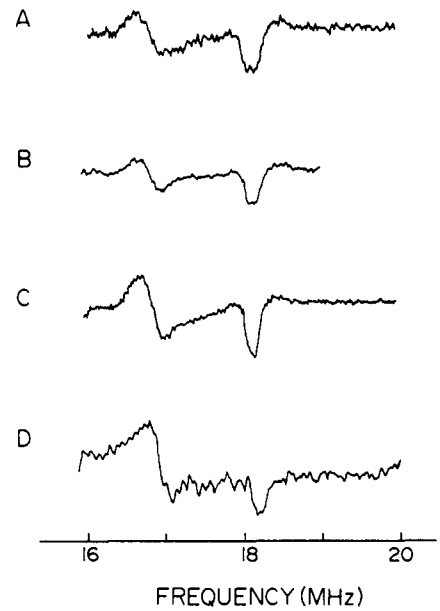

Figure 6. Expanded plots of the ENDOR spectra in the region 16–20 MHz obtained from the various enzyme preparations (16× vertical expansion made using computer): (A) ribonucleotide reductase in deuterated buffer; (B) ribonucleotide reductase containing tyrosine specifically deuterated at the β-methylene posiiton; (C) ribonucleotide reductase in protonated buffer; (D) ribonucleotide reductase containing tyrosine specifically deuterated at the [3,5] positions. Note disappearance of the broad feature centered at 18.1 MHz in D.

of $|A_z|$ = 19.7 MHz and $|A_x|$ = 26.9 MHz. The transition corresponding to A_y is partially obscured by the sharp transition at 18.2 MHz; however, following deuteration at the [3,5] ring positions, a feature with a line width of approximately 1 MHz disappears (Figure 6). To this broad feature centered at 18.3 MHz we assign A_y of the [3,5] protons and obtain $|A_y|$ = 7.8 MHz. The isotropic coupling constant determined from these principal values is $|A_{iso}|$ = 18.1 MHz.

Two distinct line shapes were observed for the ENDOR transitions of the β-methylene protons, depending on the temperature at which the experiment was performed. At 100 K the line is axial (Figure 7), which is the result expected from powder ENDOR experiments.[25] At this temperature transition frequencies $\nu_\perp$ = 42.2 MHz and $\nu_\parallel$ = 44.5 MHz, corresponding to $A_\perp$ = 54.8 MHz and $A_\parallel$ = 59.4 MHz, were observed. When the temperature is

(24) (a) Hyde, J. S.; Rist, G. H.; Eriksson, I. R. *J. Phys. Chem.* **1968**, *72*, 4269. (b) Kevan, L.; Kispert, L. D. *Electron Spin Double Resonance Spectroscopy*; Wiley: New York, 1976.

(25) (a) O'Malley, P. J.; Babcock, G. T. *J. Chem. Phys.* **1984**, *80*, 3912. (b) Kwiram, A. L. *J. Chem. Phys.* **1972**, *57*, 1132. (c) Dalton, L. R.; Kwiram, A. L. *J. Chem. Phys.* **1972**, *57*, 173.

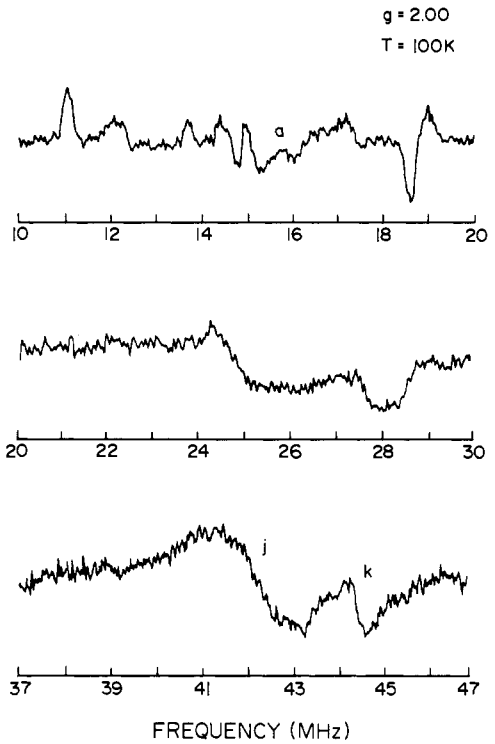

Figure 7. Proton ENDOR spectrum of ribonucleotide reductase obtained at 100 K, indicating temperature dependence of line shape. Spectrometer conditions: microwave power, 20 mW; radiofrequency power, 125 W; FM amplitude, 75 kHz. ν_p = 14.74 MHz.

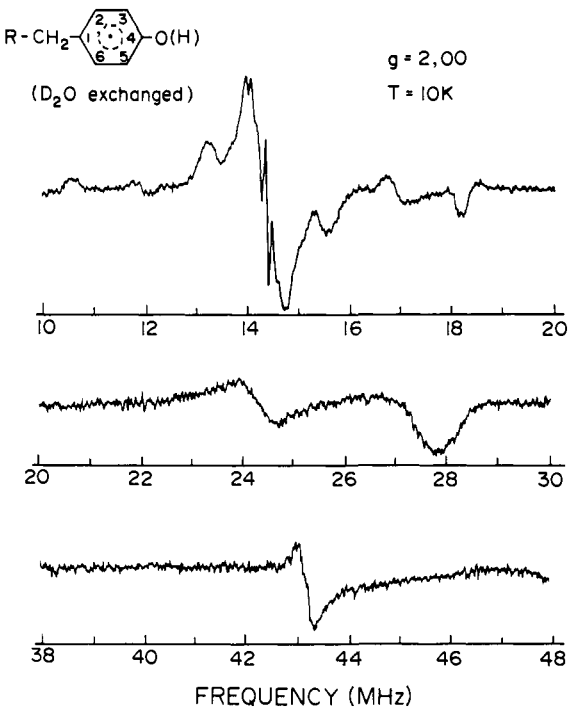

Figure 8. Proton ENDOR spectrum of ribonucleotide reductase in D_2O buffer. Lack of changes in the observed transition frequencies indicate an absence of hydrogen bond interactions. Spectrometer conditions as in Figure 3.

lowered to 10 K, the shape of the line changes (Figure 3) and features a sharp derivative-shaped component that separates two broad turning points. The sharp feature is observed at 43.2 MHz, and the turning points occur at 41.8 and 44.8 MHz. The couplings obtained from this latter set of observed transition frequencies are A_1 = 54.8 MHz, A_2 = 57.8 MHz, and A_3 = 60.8 MHz. The isotropic coupling constant for the β-methylene proton is 56.3 MHz, as determined from the axial couplings; the more rhombic-like transition observed at 10 K yields an isotropic coupling constant of 57.8 MHz. The magnitude of these couplings is consistent with the observation that the major contribution to the EPR line width is due to the β-methylene hyperfine interaction.[8a]

In the solid state, ENDOR spectra contain a prominent feature located at the Larmor frequency of the free proton. This so-called "matrix ENDOR" line is due to purely dipolar interactions between the unpaired electron and surrounding protons.[24] The presence of a matrix line in biological materials allows us to ascertain the extent to which bulk water is accessible to the radical. This test is accomplished by exchanging solvent H_2O with D_2O and looking for changes in the intensity of the matrix ENDOR line. The loss of intensity following D_2O exchange is often interpreted as a measure of solvent accessibility.[24b,26] Figure 8 illustrates the ENDOR spectrum obtained following reconstitution of protein B2 in D_2O buffer. Comparison of Figures 3 and 8 indicates a reduction of the matrix intensity as a result of exchange (note the relative intensity of the matrix line and of the nearby transitions at 18 MHz). This result implies that the tyrosyl radical of ribonucleotide reductase is accessible to bulk water to within a radius of 5–6 Å.

Hydrogen bonding interaction involving a paramagnet may be observed in the solid-state ENDOR spectrum[27] and is characterized by hyperfine interactions whose principal values comprise a traceless tensor, consistent with a purely dipolar interaction. Such interactions should be readily identified in biological systems if they are labile to exchange with D_2O. In our experimental results there are no apparent dipolar couplings in the "close coupling" range ($|A|/2$ less than 5 MHz) that are susceptible to the D_2O exchange procedure used, and we infer that under our experimental conditions we observe no hydrogen bonding interactions.

In the close-coupling range nearly axial-shaped features are observed and labeled as b and c in Figure 3. These lines are insensitive to all deuteration experiments. The parameters obtained from these transition frequencies indicate that the hyperfine tensor is not traceless, and therefore that they do not arise from purely dipolar interactions. These data preclude assignment to a hydrogen bond; however, the couplings do compare favorably with the isotropic hyperfine couplings obtained from solution spectra of tyrosyl and phenoxy radicals for ring protons at the meta positions.[28] We therefore make the assignment of these features of the [2,6] protons.

In the wings of the matrix region we resolved a second set of couplings. At 100 K the large featureless matrix line collapses, revealing a pair of axial lines that are labeled a in Figure 7. These same couplings were also resolved from the matrix line in a g-orientation selection measurement (Figure 9). In these latter experiments, orientation-dependent enhancements in the ENDOR spectrum are observed by selecting certain regions within the powder EPR spectrum whose corresponding ENDOR is defined by the orientation of the paramagnet with respect to the external field.[24,25a,27a,29] Taking the ENDOR spectrum at several g values, we are able to enhance the resolution of certain couplings whose tensor components align along the selected field.

At g = 1.99 the matrix line is highly resolved and a nearly axially symmetric set of resonances whose principal values are −1.9, −2.3, and +4.2 MHz is observed. The absolute signs of these

(26) (a) Eriksson, L. E. G.; Hyde, J. S.; Ehrenberg, A. *Biochim. Biophys. Acta* **1969**, *192*, 211. (b) Eriksson, L. E. G.; Ehrenberg, A.; Hyde, J. S. *Eur. J. Biochem.* **1970**, *17*, 539.

(27) (a) O'Malley, P. J.; Babcock, G. T. *J. Am. Chem. Soc.* **1986**, *108*, 3995. (b) Gloux, P.; Lamotte, B. *Mol. Phys.* **1972**, *24*, 23.

(28) (a) Sealy, R. C.; Harman, L.; West, P. R.; Mason, R. P. *J. Am. Chem. Soc.* **1985**, *107*, 3401. (b) Fasanella, E. L.; Gordy, W. *Proc. Natl. Acad. Sci. U.S.A.* **1969**, *62*, 299. (c) Stone, T. J.; Waters, W. A. *J. Chem. Soc.* **1964**, 213. (d) Dixon, W. T.; Murphy, D. *J. Chem. Soc., Faraday Trans. 2* **1976**, *72*, 1221. (e) Dixon, W. T.; Moghimi, M.; Murphy, D. *J. Chem. Faraday Trans. 2* **1974**, *70*, 1713. (f) Box, H. C.; Budzinski, E. E.; Freund, H. G. *J. Chem. Phys.* **1974**, *61*, 2222.

(29) Eriksson, L. E. G.; Ehrenberg, A. *Biochim. Biophys. Acta* **1973**, *293*, 57.

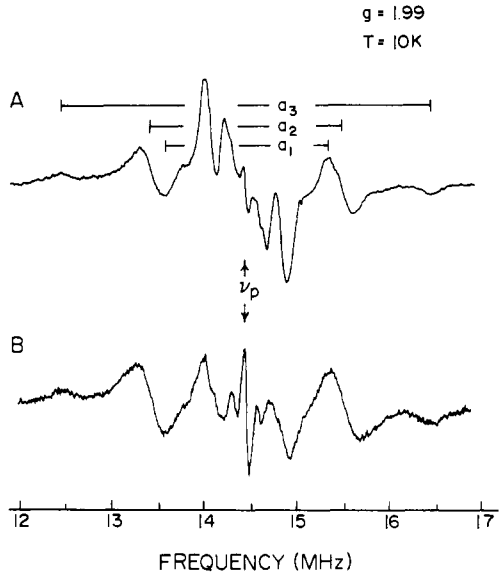

Figure 9. Enhanced-resolution single-crystal-like ENDOR spectrum in the close coupling region obtained by *g*-orientation selection: (A) ribonucleotide reductase in protonated Tris buffer; (B) ribonucleotide reductase in D_2O buffer. Spectra contain dipolar couplings not attributable to a hydrogen bond (due to lack of effect from solvent deuteration). Spectrometer conditions: microwave power, 0.5 mW; radiofrequency power, 50 W; FM amplitude, 10 kHz. ν_p = 14.42 MHz. T = 10 K.

tensor components are assigned on the assumption that they are the result of dipolar interactions, which requires that the tensor be traceless. The result of the same experiment performed on the D_2O exchanged enzyme is also shown (Figure 9B). Although the matrix transitions have become less intense, the near-axial line remains. From this result we infer that these coupling are not the result of hydrogen bonding interactions. In the previous analysis of the EPR spectrum of ribonucleotide reductase, it was shown that the orientations of the two β-methylene protons relative to the tyrosine phenol ring are not equivalent.[8a] One of the β protons was determined to reside at a dihedral angle of approximately 30° with respect to the C-1 p_z orbital, whereas the second β proton was postulated to be situated in the plane of the ring. Since the principal interaction responsible for the hyperfine coupling of β protons is hyperconjugation, this latter proton would be expected to have a near-zero contact term, and therefore dipolar terms should dominate. For this reason we assign these couplings to the β proton whose dihedral angle is near 90°.

Discussion

α-Proton Couplings. In a previous study of the EPR spectra obtained from the ribonucleotide reductase tyrosyl radical, an isotropic hyperfine coupling of 21 MHz was deduced and used to assign a spin density of 0.26 to ring carbons C-3 and C-5.[8a] The present ENDOR data confirm the isotropic hyperfine coupling value and extend the information that can be obtained with the specifically deuterated samples. This improvement is derived from the ability of ENDOR to resolve the anisotropic components of the hyperfine tensor from powder samples. Estimating the spin density by using the McConnell relation is a procedure that suffers from uncertainties associated with the selection of the proportionality constant Q. This is because Q values reported for the α protons of aromatic radicals span a range of several MHz. Having the anisotropic components available allows us to determine the spin density distribution in a way that avoids potential errors that may arise in using the simple McConnell relation and an arbitrarily chosen value for the parameter Q.

The dipolar contributions to the observed hyperfine couplings arise from the interaction of the nucleus in question with the unpaired spin density delocalized throughout the parent aromatic ring. Taking the observed couplings of the [3,5] protons as negative (cf. ref 30), the dipolar terms are determined to be.

$$A_{\mu x} = -8.8 \text{ MHz}; A_{\mu y} = +10.3 \text{ MHz}; A_{\mu z} = -1.6 \text{ MHz}$$

Table II. Dipolar Hyperfine Couplings[a] of H-3(5) and H-2(6) with the Electron Spin Density Localized on Nuclei of the Aromatic Ring

atom	R (Å)[b]	angle[b]	ρ	$A_{\mu x}$	$A_{\mu y}$	$A_{\mu z}$
			H-3(5)			
C-1	3.41	−22.0	0.49	−0.90	1.67	−0.77
C-2(6)	2.14	−34.7	−0.07	0.47	−0.77	0.30
C-3(5)	1.09	0.0	0.26	−8.46	8.62	−0.15
C-4	2.16	34.2	−0.03	0.20	−0.33	0.13
C-5(3)	3.42	22.0	0.26	−0.48	0.88	−0.40
C-6(2)	3.87	1.1	−0.07	0.09	−0.17	0.08
O-1	2.67	64.8	0.16	−0.59	1.04	−0.45
			H-2(6)			
C-1	2.16	−34.4	0.49	−3.21	5.32	−2.11
C-2(6)	1.09	0.0	−0.07	2.51	−2.51	−0.02
C-3(5)	2.15	34.7	0.26	−1.72	2.85	−1.13
C-4	3.39	21.3	−0.03	0.06	−0.11	0.05
C-5(3)	3.84	0.0	0.26	−0.34	0.64	−0.30
C-6(2)	3.39	−20.3	−0.07	0.13	−0.25	0.12
O-1	4.15	38.7	0.16	−0.17	0.30	−0.13

[a] Tabulated hyperfine components are principal values of individual dipolar interactions between designated proton and the localized spin density. The total dipolar tensor reported in the text is the resultant obtained by rotating each of these diagonal tensors by the indicated angle into a coincident reference frame, summing these rotated tensors, and diagonalizing the sum. [b] Determined from neutron diffraction structure: Frey, M. N., et al. *J. Chem. Phys.* **1973**, *58*, 2547.

These three components represent the total dipolar tensor for the [3,5] protons, which is a sum of the dipolar tensors for the interaction between H-3(5) and the spin density on each of the nuclei in the aromatic system.[27a,31] The spin density on the aromatic ring can be deduced by calculating the individual dipolar terms, rotating the resultant tensors onto a common reference frame, and summing. The quality of the calculated spin density distribution is assessed by the accuracy of the fit between the calculated and observed dipolar tensor.

The procedure for determining the spin density distribution for the ribonucleotide reductase tyrosyl radical is based on the method outlined by Heller and Cole,[31a] and used previously by O'Malley and Babcock in an analysis of the ENDOR spectrum of *p*-benzosemiquinone.[27a] The geometric parameters (distance over which the interaction occurs, and the angle of rotation of the y axis) were determined from the neutron diffraction structure of L-tyrosine.[32] As an initial guess for the spin density distribution, we made the assumption that the radical is a seven-member odd-alternate aromatic (cf. ref 30), and used spin density distributions reported for tyrosyl and phenoxy radicals.[8a,28] That the tyrosyl radical can be regarded as an odd-alternate system is suggested by the reported spin density distributions cited above and an SCF calculation by Fasanella and Gordy that was included in their single-crystal EPR study of tyrosine·HCl.[28b] We then optimize the spin density distribution by an iterative process of varying the spin density distribution and comparing the fit of the resultant [3,5] hyperfine tensor to our experimental result.

Table II lists the optimized spin densities and individual components for the dipolar interactions of the ring protons (both H-3(5) and H-2(6)) based on a fit of the calculated total dipolar tensor to experiment. A large positive spin density is predicted for C-1(0.49), C-3(5) (0.26), and the oxygen (0.16). These results are consistent with the previously reported C-1, C-3, and C-5 spin densities determined from EPR measurements,[8a] and the suggestion made here that the tyrosyl approximates an odd-alternate aromatic. In the earlier EPR report[8a] the spin density on carbons C-2, C-4, and C-6 was estimated to be less than 0.15; our present results allow us to assign a spin density of −0.03 to carbon C-4, and −0.07 to carbons C-2 and C-6. The change in sign of the

(30) Wertz, J. E.; Bolton, J. R. *Electron Spin Resonance: Elementary Theory and Practice*; McGraw Hill: New York, 1972.
(31) (a) Heller, C.; Cole, T. *J. Chem. Phys.* **1962**, *37*, 243. (b) Hirota, N.; Hutchinson, C. A.; Palmer, P. *J. Chem. Phys.* **1964**, *40*, 3717. (c) Bohme, U. R.; Wolfe, H. C. *Chem. Phys. Lett.* **1972**, *17*, 582.
(32) Frey, M. N.; Koetzle, T. F.; Lehmann, M. S.; Hamilton, W. C. *J. Chem. Phys.* **1973**, *58*, 2547.

Table III. Comparison of Calculated and Experimentally Observed Hyperfine Tensor Components

	calculated			experimental		
proton	A_x	A_y	A_z	A_x	A_y	A_z
H-3(5)	−26.9	−8.0	−19.4	−26.9	−7.8	−19.7
H-2(6)	+8.1	+5.2	+1.4	+7.6	+4.8	
H_{β_2}	−2.9	+4.9	−1.9	−2.3	+4.2	−1.9

unpaired spin density at the [2,6] carbons relative to the [3,5] protons is typically observed for the spin density distribution in phenoxy model compounds.[28c-e] The total dipolar hyperfine tensor calculated by using this spin density distribution is

$$\mathbf{A}_{\mu x} = -8.8 \text{ MHz}; \mathbf{A}_{\mu y} = +10.1 \text{ MHz}; \mathbf{A}_{\mu z} = -1.3 \text{ MHz}$$

for the [3,5] protons, in excellent agreement with the experimental values above (see Table III). From the measured isotropic coupling (−18.1 MHz) and the calculated spin density of the [3,5] protons we determine that Q is −69.6 MHz, which is within the range of literature values of Q's determined for C–H fragments of aromatic radicals (cf. ref 30).

We observed hyperfine couplings of $|A_1| = 4.8$ MHz and $|A_2| = 7.6$ MHz, and have assigned these to the [2,6] protons. An empirical relationship has been reported for the α-proton isotropic hyperfine couplings of p-phenoxy radicals;[26e] according to this rule, $|A_{\text{meta}} + A_{\text{ortho}}| = 13.2 \pm 0.2$ MHz. If we substitute into this equation the experimentally determined A_{ortho} of ribonucleotide reductase, we obtain for the isotropic coupling of the [2,6] protons a value of $+4.9 \pm 0.2$ MHz. This value coincides closely with an observed hyperfine component assigned to the [2,6] protons, and is consistent with a spin density of −0.07 as predicted from the dipolar calculations described above for the [3,5] protons.

The lower half of Table II lists the parameters and results of calculations performed for the dipolar tensor components of the C-2 and C-6 protons. The total dipolar tensor determined for these protons from the individual components listed in Table II is

$$\mathbf{A}_{\mu x} = +3.2 \text{ MHz}; \mathbf{A}_{\mu y} = +0.3 \text{ MHz}; \mathbf{A}_{\mu z} = -3.5 \text{ MHz}$$

which, when summed with the isotropic component (+4.9 MHz) obtained by using the empirical rule, gives a hyperfine tensor of

$$\mathbf{A}_x = +8.1 \text{ MHz}; \mathbf{A}_y = +5.2 \text{ MHz}; \mathbf{A}_z = +1.4 \text{ MHz}$$

with an error range of ±0.2 MHz. Our calculated couplings therefore coincide with the observed data since a line shape is predicted that would appear to be axial due to one component becoming "lost" in the matrix. We could include nuclear–nuclear dipolar interactions in these calculations of the [2,6] proton couplings; however, this interaction only adds a term of the order of 0.1 MHz. The calculation of the [2,6] proton couplings provides strong support for the spin density distribution deduced above because we have used the spin density derived from the [3,5] proton couplings to predict successfully the [2,6] proton couplings. A comparison of calculated and observed hyperfine principal values based upon this spin density is presented in Table III.

Triple resonance affords us a means to determine the signs of the [2,6] proton couplings, and therefore verify our predicted values based on the analysis of the spin density distribution. With the radio-frequency "pump" at the low frequency component of the transition labeled b in Figure 3 (i.e., 11.87 MHz), we observed a triple enhancement of the high-frequency components of b and c. This result confirms that couplings associated with transitions b and c have the same absolute sign. In the same spectrum we also observed that the transitions corresponding to the [3,5] α protons were enhanced in a manner opposite to those of the [2,6] protons; that is, the low-frequency components of transitions labeled d, e, and f in Figure 3 were enhanced. These latter data indicate that the signs of the hyperfine tensor components of the [2,6] α protons are opposite to those of the [3,5] protons.

β-Methylene Proton Couplings. The transition observed at approximately 43 MHz corresponds to the high-frequency transition of the β proton (i.e., $|A|/2 + \nu_p$). Although we do not observe a second set of ENDOR lines located at a frequency $2\nu_p$ greater or less than the transitions at 43 MHz, we make the above assignment based on the earlier EPR results, which showed that the isotropic hyperfine coupling of the β proton is approximately 50 MHz.[14]

The lines corresponding to the low-frequency ENDOR transitions for this strongly coupled β-methylene proton are predicted to occur near the matrix region; however, none are observed that may be attributed to a near-axial tensor for a β proton. These features could be obscured by the matrix, although there are no lines resolved in either the D_2O exchanged, g-oriented, or 100 K spectra (cf. Figures 7–9). The collapse of one of the ENDOR transitions may be attributable to the domination of cross-relaxation processes, or to simple hyperfine enhancement of the higher energy set of NMR transitions. Spin exchange, on the other hand, affects both spin α and spin β states, and, in general, the net effect is a loss of enhancement across the entire spectrum (cf. ref 24b and 33).

At 10 K it is possible that the cross-relaxation time is shorter than the electron spin–lattice relaxation time. We observed that the ENDOR spectrum of the β protons is not altered by saturating different regions of the EPR spectrum; this result is consistent with the proposed relationship between the two relaxation rates.[25c] Modulation of the isotropic coupling is a mechanism that can enhance cross-relaxation rates and lead to intensity changes in ENDOR spectra.[34] Modulation of the dihedral angle of a β-proton would provide a periodic alteration of the contact interaction; however, it is unlikely that the rate of tunneling at 10 K between equivalent rotational conformers is sufficient to provide the necessary modulation. On the other hand, the iron pair in protein B2 provides a second spin system that can engage in cross relaxation with the tyrosyl radical independent of spin exchange.[5c] The iron pair interacts with the tyrosyl radical via dipolar coupling, and through this interaction cross relaxation is rendered possible.[35] However, this mechanism is not effective below 30 K because of the low population of the paramagnetic state of the iron center at these temperatures.[5c] We conclude, then, that hyperfine enhancement is the principal mechanism responsible for the dominance of the high-frequency ENDOR transitions for the β protons.

The rotational conformation of the tyrosyl radical about the C-1 to C-β bond can be determined from the isotropic coupling of the β-methylene proton. In radicals of the type $Ar^{\bullet}-CH_2-R$, the couplings of the β-methylene protons are angle dependent, and the effect is expressed in terms of a modified form of the McConnell relation. For β protons Q becomes a function of molecular geometry, i.e.

$$Q(\theta) = \mathbf{B}_0 + \mathbf{B}_1 \cos^2 \theta$$

where θ is the dihedral angle defined by the p_z orbital on the adjacent carbon on the aromatic ring and the $C_\beta-H_\beta$ bond.[36] For practical applications B_0 is neglected because it is much smaller than B_1. The resultant angle-depdendent McConnell relation is then

$$\mathbf{A}_{\text{iso}} = \mathbf{B}_1 \rho \cos^2 \theta$$

From our ENDOR spectra we have determined that A_{iso} for this β proton (H_{β_1}) is 56.3 MHz and that the spin density on C-1 is 0.49. B_1 has been determined to be 162 MHz for β protons[37] and was previously applied to the tyrosyl radical by Fasanella and Gordy.[28b] These data yield a θ of 33° (cf. Figure 10, right), consistent with the previous EPR analysis,[14] which indicated that θ_1 was approximately 30°.

(33) Freed, J. H. *J. Phys. Chem.* **1967**, *71*, 38.
(34) Atherton, N. M. In *Multiple Electron Resonance Spectroscopy*; Dorio, M. M., Freed, J. H., Eds.; Plenum Press: New York, 1979.
(35) Freed, J. H. In *Electron Spin Resonance in Liquids*; Muus, L. T., Atkins, P. W., Eds.; Plenum Press: New York, 1972; p 387. Owen, J.; Harris, E. A. In *Electron Paramagnetic Resonance*; Geschwind, S., Ed.; Plenum Press: New York, 1972; p 427. Poole, C. P.; Farach, H. A. *Relaxation in Magnetic Resonance*; Academic Press: New York, 1971.
(36) Derbyshire, W. *Mol. Phys.* **1962**, *5*, 225. Stone, E. W.; Maki, A. H. *J. Chem. Phys.* **1962**, *37*, 1326.
(37) Fessenden, R. W.; Schuler, R. H. *J. Chem. Phys.* **1963**, *39*, 2147.

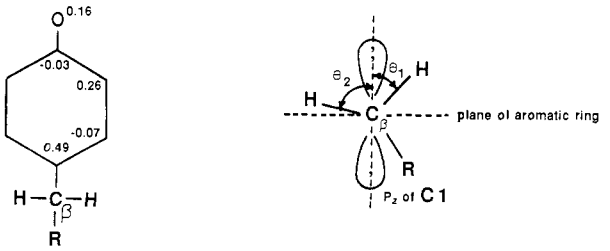

Figure 10. Model of the tyrosyl radical of ribonucleotide reductase based upon the ENDOR data: left, spin density distribution; right, end on view along the C_1–C_β bond showing θ_1, θ_2, and the orientation of the β-methylene protons.

Our ENDOR spectra also support the previous suggestion that the second β proton (H_{β_2}) is situated in the plane of the aromatic ring ($\theta_2 \cong 90°$), as the occurrence of weak transitions insensitive to D_2O exchange is expected for the second β proton in such a geometry. Again, using the geometry of L-tyrosine,[32] we can estimate the principal hyperfine components for the dipole–dipole interaction involving this β-methylene proton. Taking the C_β–H_{β_2} bond length as 1.09 Å, the distance over which the dipolar interaction between H_{β_2} and spin density on C-1 occurs is 2.14 Å. The dipolar tensor computed by the McConnell-Strathdee method[38] for this interaction is then

$$A_{\mu x} = -2.9 \text{ MHz}; \; A_{\mu y} = +4.9 \text{ MHz}; \; A_{\mu x} = -1.9 \text{ MHz}$$

Although the terms corresponding to the interaction within the plane of the ring are higher than the observed couplings, the agreement of the computed values to experiment is adequate to support the assignment of these couplings to the β proton situated in the ring plane. Neglected in this computation are the corrections arising from additional dipolar terms such as the interaction between H_{β_2} and the spin density on the other carbons of the aromatic ring, and the nuclear-nuclear couplings with B_{β_1} and H-2(6). Including the electron-nuclear term for the proton and its next nearest neighbor (C-2 or C-6) decreases the magnitude of each term by approximately 100 kHz, and the correction from the nuclear–nuclear term reduces the coupling by another 50 kHz. A larger decrease in the magnitude of the x and y components is achieved if the interaction distance is increased, which is possible given the fact that the neutron scattering data were obtained for the nonradical form of the molecule, by either increasing the C–H bond length or rotating the β proton slightly out of the plane of the ring. The latter option is already suggested from the analysis above of the large β-proton coupling.

A similar calculation can be used to argue against the assignment of these small dipolar couplings to hydrogen bond interactions. With an estimated spin density on the oxygen of approximately one-third that of C-1, estimated couplings to a hydrogen bonded proton are less than half the observed values.

Model for the Tyrosyl Radical of Ribonucleotide Reductase. Figure 10 shows the geometry and spin density distribution we deduce for the tyrosyl radical of ribonucleotide reductase. Unpaired electron spin density is localized on carbons C-1, C-3, and C-5 of the aromatic ring. There is also significant spin density on the phenolic oxygen, and a spin density distribution model of the odd-alternate type fits the experimental data well. Carbons C-2, C-4, and C-6 all have slightly negative spin density. The magnitudes of the hyperfine couplings of the β protons indicate that one of these protons interacts strongly with the p orbital on C-1. The other β proton lies close to the plane of the ring and is geometrically prevented from any substantial interaction with the C-1 orbital.

As is evident from Figure 10, we propose that the tyrosyl radical of protein B2 is uncharged and lacks interaction with hydrogen bonding protons. Our evidence for this comes from the D_2O exchange experiments and from recently published resonance Raman data.[6,20] In these latter studies the resonance Raman spectra, obtained with excitation close to the 410-nm absorption maximum of the tyrosyl radical, yielded a strongly enhanced mode at approximately 1500 cm^{-1}, which was interpreted as the C–O stretch of a deprotonated tyrosyl radical.[6,39] The assignment of the tyrosyl radical of ribonucleotide reductase as a neutral species is also consistent with its absorption maximum at 410 nm[5a,6,3,39] and its g_{iso} of 2.0047.[11,19] The estimated isotropic g value for the tyrosyl radical in ribonucleotide reductase is consistent with the g_{iso} of neutral radicals (typically 2.0046) and differs from those that are usually found for protonated radicals (2.0033).[28d,40]

From an earlier study on the relative reactivity of the tyrosyl radical toward more or less bulky hydroxamic acid analogues, it was concluded that the tyrosyl radical of *E. coli* protein B2 is buried in a cleft that is about 4 Å wide and at least 6 Å deep.[41] This is consistent with our present finding that the radical of protein B2 is accessible to bulk water within approximately that range. Under our experimental conditions we could not observe any hydrogen bonding interactions between the tyrosyl radical and bulk water or solvent exchangeable protons in the cleft. The generation of the tyrosyl radical, which involves an oxidation, may in fact be greatly facilitated in the deprotonated state, as has been shown earlier to be the case for tyrosine in solution.[42] Since all available data suggest that the reaction mechanism catalyzed by ribonucleotide reductase is initiated by a tyrosyl radical mediated 3 hydrogen abstraction from the substrate, a deprotonated, nonhydrogen bonded tyrosyl radical would be the most obvious candidate.[1,2,28a,43]

The data presented here for the tyrosine radical in ribonucleotide reductase contrasts with those we have obtained for the tyrosine radicals that occur in photosystem II in plant and algal photosynthesis: the former is present as a neutral nonhydrogen bonded species; the latter, while still neutral radicals, as indicated by their g values and hyperfine coupling constants,[40] form hydrogen bonds to proton donors in the local protein environment. The protein milieu undoubtedly plays a substantial role in directing the properties of these two different types of tyrosyl radicals to their specific functions. We have domonstrated here that EPR and ENDOR spectroscopies are well suited to elucidate such specific protein/radical contacts, particularly those that control the orientation of the phenol head group with respect to the polypeptide backbone and those that influence hydrogen bond interactions to the phenol oxygen. These may be the preferred techniques for elucidating the microenvironment of similar radical species, e.g., the recently demonstrated catalytically important tyrosyl radical in prostaglandin H synthase.[13]

Acknowledgment. This research was supported by the National Institutes of Health (GM-37300; GTB), and the Swedish Medical (B.M.S.) and Natural Science Research Councils (B.M.S., A.E., and L.P.).

(38) McConnell, H. M.; Strathdee, J. *Mol. Phys.* **1959**, *2*, 129.
(39) Tripathi, G. N. R.; Schuler, R. H. *J. Chem. Phys.* **1984**, *81*, 113.
(40) Barry, B. A.; Babcock, G. T. *Chem. Scr.* **1988**, *28A*, 117.
(41) Kjøller Larsen, I.; Sjöberg, B.-M.; Thelander, L. *Eur. J. Biochem.* **1982**, *125*, 75.
(42) Harriman, A. *J. Phys. Chem.* **1987**, *91*, 6102.
(43) Ator, M.; Stubbe, J.; Kenitsky, T. *J. Biol. Chem.* **1983**, *258*, 1625.